Slow Slip Events Following the 2002 Mw 7.1 Hualien Offshore Earthquake Afterslip

Sean Kuanhsiang Chen (sean80254@gmail.com)
National Taiwan University https://orcid.org/0000-0002-6112-1282
Yih-Min Wu
National Taiwan University
Yu-Chang Chan
Academia Sinica

Full paper

Keywords: slow slip events, afterslip, coseismic and postseismic stress perturbation, Coulomb stress change

Posted Date: April 28th, 2021

DOI: https://doi.org/10.21203/rs.3.rs-450720/v1

Abstract

The recurrence intervals of slow slip events may increase gradually after a large earthquake during the afterslip. Stress perturbations during coseismic and postseismic periods may result in such an increase of intervals. However, the increasing recurrence intervals of slow slip events are rarely observed during an afterslip. The evolution process along with the afterslip remains unclear. We report an observation of slow slip events following the 2002 M_w 7.1 Hualien offshore earthquake afterslip in the southernmost Ryukyu subduction zone. Slow slip events in 2005, 2009, and 2015 are adjacent to the M_w 7.1 earthquake hypocenter. An increasing slow-slip interval of 3.1, 4.2, and 6.2 years has been observed after the earthquake. We calculated coseismic and postseismic slips from the M_w 7.1 earthquake and then estimated the Coulomb stress changes in the slow slip region. The M_w 7.1 earthquake has contributed positive Coulomb stresses to both the 2005 slow-slip region and 2009/2015 repeating slow-slip region. The coseismic and postseismic Coulomb stress change on the 2005 slow-slip region is approximately 0.05 MPa and 0.035 MPa, respectively. However, both Coulomb stress changes on the 2009/2015 repeating slow-slip region are not over 0.03 MPa. The ongoing afterslip following the M_w 7.1 earthquake last for at least five years, evolving with a decaying stress rate with time. The long-term stress perturbations may be able to trigger the 2005 slow slip event during the afterslip. The 2009 slow slip event seems to be influenced by the afterslip as well. Postseismic stress evolution and frictional and stressed conditions of the slow-slip region can be a reason to affect the evolution process of slow slip events intervals.

Introduction

Slow slip events (SSEs) in subduction zones usually occur on the downdip/updip ends of the seismogenic zone or the adjacent sides (e.g., Bürgmann 2018; Rogers and Dragert 2003; Schwartz and Rokosky 2007). The close spatial distance from SSEs to the seismogenic zone raises a question: whether large earthquakes can affect the recurrence intervals of the nearby SSEs. The SSE recurrence intervals keep constant approximately between two large earthquakes and the constant increases with the duration time of SSEs (e.g., Matsuzawa et al. 2013; Obara and Kato 2016; Ozawa et al. 2007). Numerical modeling results suggest that SSE recurrence intervals will be shortened after a large earthquake and then increase gradually with time, recover to the constant (e.g., Luo and Liu 2019; Matsuzawa et al. 2010; Segall and Bradley 2012). The shortening of one SSE recurrence interval has been observed after large earthquakes immediately, triggered by coseismic dynamic stresses from the passing seismic waves (Katakami et al. 2020; Wallace et al. 2017; Wei et al. 2018). However, the observation in nature similar to those numerical modeling results is very rare. Recently, increasing recurrence intervals of SSEs are detected after the 2011 M_w 9.0 Tohoku earthquake in the Boso region, Japan (Hirose et al. 2012; Luo and Liu 2019; Ozawa et al. 2019). The recurrence intervals before the Tohoku earthquake are approximately 4 to 6 years, which shortens to 0.6, 2.2, and 4.4 years after the earthquake (Ozawa et al. 2019). Stress perturbations during coseismic and postseismic periods can be a reason for the increasing recurrence intervals of the Boso SSEs. Coseismic stress perturbations, either the dynamic or static types sustained

only a short period during the coseismic slip. Afterslip usually accompanies a long-time postseismic stress perturbation. It may thus be the dominant influence in the increasing recurrence intervals of SSEs. The argument remains unsure because another SSEs sequence in Costa Rica has demonstrated a counterexample. The recurrence intervals of the Costa Rica SSEs before the 2012 M_w 7.6 Nicoya earthquake are approximately 1.8 to 2.0 years that did not change after the earthquake (Voss et al. 2017; Xie et al. 2020). Besides, the Kapiti SSEs sequence in New Zealand is well-recorded with a long history as well. The recurrence intervals before the 2016 M_w 7.8 Kaikōura earthquake are approximately 5.0 years, have been shortened to 0.5 years after the Kaikōura earthquake (Shibazaki et al. 2019; Wallace et al. 2018). This observation has a chance to support the Boso SSEs study if the future Kapiti SSEs keep the increasing recurrence intervals with time. So far, the influence of afterslip on SSEs recurrence intervals remains unclear.

The southernmost Ryukyu subduction zone has converged rapidly at 12.5 cm/yr in the N-S direction (Hsu et al. 2012), which includes a 5.0 cm/yr southward back-arc spreading from the Okinawa Trough (Nishimura et al. 2004). Whereas, magnitudes of the large earthquakes did not exceed M_w 7.7 over the last 300 years (Cheng and Yeh 1989; Theunissen et al. 2010). The most recent large one was the 2002 M_w 7.1 earthquake located in the offshore Hualien area at approximately the depth of 16 km (Fig. 1a). In this subduction, we report an observation of SSEs sequence in 2005, 2009, and 2015 following the 2002 M_w 7.1 Hualien offshore earthquake afterslip. The 2005 SSE may have nucleated near the updip region of the M_w 7.1 earthquake, and the 2009 and 2015 SSEs occurred near the downdip region (Fig. 1a). The SSEs are adjacent to the M_w 7.1 earthquake hypocenter with increasing intervals of 3.1, 4.2, and 6.2 years after the earthquake (Fig. 1b). The observation points out an important question. Whether stress perturbations during coseismic and postseismic periods of the M_w 7.1 earthquake can affect the SSEs intervals? To this end, we calculated the coseismic and postseismic slips from the M_w 7.1 earthquake in the subduction zone. Then Coulomb stress changes are estimated based on both the slips on the SSEs region. The Coulomb stress changes were examined to identify whether they were sufficient for an increase of SSE intervals. We find that SSE regions were very likely overlapped by the afterslip region of the M_w 7.1 earthquake. The 2005 SSE region has been imposed by higher positive Coulomb stresses than the 2009/2015 SSEs region. The afterslip lasted from 2002 April to at least early 2007 with a time-decaying stress rate. The continuous positive stress loads may be sufficient for the triggering of 2005 SSE and affect the 2009 SSE. Our study provides an observation of SSEs sequence following afterslip that can support the Boso SSEs case.

Tectonic background of the southernmost Ryukyu subduction zone

In the southernmost Ryukyu subduction zone, the Philippine Sea Plate subducts northward beneath the Eurasian Plate to form the back-arc rifting (Sibuet et al. 1987). At the southernmost end, the Eurasian Plate subducts eastward beneath the Philippine Sea Plate at the Taiwan orogen; the convergence rate is approximately 8.0 cm/yr in the 310° direction (e.g., Chen et al. 2014, 2017; Hsu et al. 2009). There is an additional 5.0 cm/yr southward spreading from the Okinawa Trough. Thus, the N-S direction convergence

rate reaches 12.5 cm/yr between the Ryukyu Trench and the Yonaguni Island (Fig. 1a). Three areas have been proposed on this subduction interface: (1) the Interplate Seismogenic Zone (ISZ; Kao 1998), (2) Ryukyu Fault (Hsu et al. 2012), and (3) Slow Slip Zone (SSZ; Chen et al. 2018). The ISZ is a seismogenic zone that many earthquakes are with magnitudes greater than M_w 5.0. This zone is between the Ryukyu Trench and the Yonaguni Island at depths of approximately 20–40 km (Fig. 1a). The 2002 M_w 7.1 Hualien offshore earthquake was situated at the western end of the ISZ and above its interface in the overriding plate (Fig. 1a). The M_w 7.1 earthquake was less studied due to the lack of near-field observations, only for the coseismic displacement (Chen et al. 2004), seismic wave propagation (Lee et al. 2009), and afterslip (Nakamura 2009). The afterslip may have lasted over five years and leads to long stress perturbations in the subduction zone. The Ryukyu Fault is a locked region where megathrust earthquakes might occur (Hsu et al. 2012). The locked dimension remains unclear, estimated by only the Global Navigation Satellite System (GNSS) observations in the eastern Taiwan orogen. If the dimensions reached the maximum value (Fig. 1a), the magnitude of the earthquake would be $7.5 \leq M_w \leq 8.7$ (Hsu et al. 2012). The longer the earthquake cycle is, the larger the earthquake size will be. The SSZ is an SSE region next to the Taiwan orogen where SSEs occurred in 2005, 2009, and 2015 at depths of approximately 15–45 km (Chen et al. 2018). SSEs in this region were difficult to be identified before the 2002 M_w 7.1 Hualien offshore earthquake because the onshore GNSS observations were limited (Fig. 2). Current GNSS observations revealed that 2005 SSE might have occurred on the Ryukyu Fault. Some SSEs have been observed coexisting in the seismogenic zone or the locked region (e.g., Dixon et al. 2014; Ito et al. 2013). The 2009 and 2015 SSEs recurred on the same patch near the downdip end of Ryukyu Fault as regarded as repeating SSEs. The three SSEs lasted from 2 to 4 months with a potential maximum size, M_w 6.4 to 6.6. The SSEs were likely originated from a high V_P/V_S ratio zone on the subduction interface (Huang et al. 2014) and are accompanied by overriding plate seismicity with maximal magnitudes greater than M_w 5.0. The peak slip of the three SSEs is adjacent to a high b-value region in the northeastern Taiwan orogen (Wu et al. 2018). A state of low differential stress may thus appear in that region (Scholz 2015). These observations agree with a broad consequence of SSEs that usually occur in the state of rich high-pressure fluids, low effective stress, and transitional friction (e.g., Bürgmann 2018; Saffer and Wallace 2015; Schwartz and Rokosky 2007). The close distances from the SSEs to the M_w 7.1 earthquake allow us to investigate the relation between afterslip and SSE intervals.

Data And Methods

To answer the questions raised in this study, we calculated Coulomb stress changes from the 2002 M_w 7.1 Hualien offshore earthquake coseismic and postseismic slips. Coseismic and postseismic Coulomb stress change can commonly explain the triggering of spatiotemporally neighboring earthquakes around a mainshock (e.g., King et al. 1994; Stein 1999). However, there were no near-field GNSS observations around the M_w 7.1 earthquake (Fig. 1a). We made assumptions for the calculations of the coseismic and postseismic slips. First, the coseismic slip was calculated on a single fault in the subduction zone by far-field GNSS coseismic displacements (Chen et al. 2004). Strike and dip of the fault are 277° and 44°

(northward), respectively, constrained by earthquake focal mechanism in a relocated earthquake catalog (Wu et al. 2008). An elastic half-space dislocation model (Okada 1992) was used to invert the coseismic displacements with the rigidity of 30 GPa. The fault dimension was initially presumed to be 50 x 30 km (Lee et al. 2009) and then optimized by grid search for the geometrical parameters. This method minimized the residuals between observed GNSS and modeled displacements. The two components of the fault dislocation vector were estimated by the least-squares. Second, the postseismic displacements following the M_w 7.1 earthquake were determined from the same far-field GNSS observations. The data are derived from the northeastern Taiwan region and Yonaguni Island (Fig. 1a), collected by the Institute of Earth Sciences, Academia Sinica, Taiwan. We analyzed the GNSS time series from 1999 to 2017, which covers the timing of the 2002 M_w 7.1 Hualien offshore earthquake and the SSEs in 2005, 2009, and 2015. For the 2002 M_w 7.1 Hualien offshore earthquake, the postseismic displacements were fitted with exponential decay functions by the least-squares (Fig. 3). The postseismic slip from the M_w 7.1 earthquake was determined by the same approach as the coseismic slip determination. The postseismic slip was assumed on the same fault patch as the coseismic slip. The additional coseismic displacements on the GNSS time series (Fig. 3) caused by the other local earthquakes have been corrected. Coulomb stress changes caused by both coseismic and postseismic slips were determined using the Coulomb 3.3 software (Toda et al. 2011). Coulomb 3.3 uses the same dislocation equation (Okada 1992) to calculate the shear and normal stresses on the fault and then the Coulomb stresses. The friction coefficients in shallow subduction zones mainly range from 0.2 to 0.4 from drilling sites in Nankai Trough, Japan Trench, and Costa Rica (e.g., Ikari et al. 2018; Namiki et al. 2014). In the seismogenic zone, the friction coefficients are usually less than a peak value of 0.35 ± 0.04 along a subducting oceanic plate interface (Kaneki and Hirono 2019). Thus, we calculated the Coulomb stress changes by assuming the friction coefficient as 0.3. Note that the Coulomb stress changes could be locally positive or negative on the regions of 2005 SSE and 2009/2015 repeating SSEs. It depends on where the peak slip is located relative to the SSE regions and the slip heterogeneity. For simplification, we calculated mean stress changes from all positive and negative stress changes on the region of the 2005 SSE and 2009/2015 repeating SSEs. We discuss whether the mean Coulomb stress changes were sufficient for an increase of SSE intervals.

Results And Discussion

Fig. 4 shows the coseismic and postseismic slips of the 2002 M_w 7.1 Hualien offshore earthquake. The inferred M_w 7.1 earthquake fault plane, constrained by both focal mechanism and far-field GNSS observations, is not located on the subduction interface. The fault plane seems to extend from the interface at approximately 40 km depth to the surface. Our results show that the coseismic peak slip is roughly 4.3 m at the northwestern downdip side near the fault center (Fig. 4a). The peak-slip location can correspond to the largest coseismic displacements that appear to the northeastern Taiwan region. The coseismic slip over 1.5 m covers almost half of the fault plane and is commonly less than 1.0 m in the updip region. The postseismic displacements likely lasted from 2002 April to early 2007 in the nearest GNSS station to the epicenter (Fig. 3). The duration of afterslip is at least five years, consistent with a previous study using another GNSS station on Yonaguni Island (Nakamura 2009). Analyzing postseismic

displacements from continuous GNSS records, most of the afterslip were surrounding the region of coseismic peak slip (Fig. 4b). The peak afterslip appears at the northwestern downdip end of the fault plane with approximately 2.6 m. The peak-slip location seems closer to the 2009/2015 repeating SSEs region than that of the coseismic peak slip. The amount of the overall afterslip is 60 to 70 % percent of the coseismic slip. It is reasonable because the postseismic displacements were less than the coseismic displacements by similar amounts. Fig. 5 shows the coseismic and postseismic Coulomb stress changes caused by the 2002 M_w 7.1 Hualien offshore earthquake. We observed that the M_w 7.1 earthquake led to positive Coulomb stresses to both the 2005 SSE region and 2009/2015 repeating SSEs region. The coseismic and postseismic Coulomb stress changes on the 2005 SSE region are approximately 0.050 ± 0.017 MPa and 0.035 ± 0.021 MPa, respectively (Fig. 5a). The Coulomb stress change caused by the afterslip is smaller than that of the coseismic slip. It is mainly because the afterslip may have produced negative Coulomb stresses in the 2005 SSE region. The 2009/2015 repeating SSEs region was affected by the positive and negative Coulomb stresses simultaneously in both coseismic and postseismic scenarios (Fig. 5b). The coseismic and postseismic Coulomb stress changes are approximately 0.010 ± 0.018 MPa and 0.027 ± 0.023 MPa, respectively. Such positive stresses are much smaller than that of the 2005 SSE region. What's more, afterslip following the M_w 7.1 earthquake may last for at least five years. The postseismic stress perturbations generally evolve with a decelerated stress rate with time in nature (e.g., Wang et al. 2012; Hu et al. 2016). Recent studies have found that SSEs can be triggered by tiny stress variations that range from 0.065 MPa to 0.02 MPa caused by passing seismic waves (Katakami et al. 2020; Wallace et al. 2017; Wei et al. 2018). The triggering stress thresholds may vary with frictional and stressed conditions of the SSE region and the magnitude of the SSEs (e.g., Katakami et al. 2020). If postseismic decelerated stress after the M_w 7.1 earthquake lasts from 2002 April to at least early 2007, the stress perturbations were sufficient for the triggering of 2005 SSE during the afterslip. We suspect the 2009 SSE might be influenced by the afterslip even if the positive Coulomb stress change were lower in that region. If so, the increasing SSE intervals are likely influenced by the M_w 7.1 earthquake afterslip.

Whether SSE recurrence intervals can be affected by a nearby large earthquake is still a debated matter. So far, two well-recorded SSE sequences in the Boso region in Japan and Costa Rica have demonstrated the end members (Luo and Liu 2019; Ozawa et al. 2019; Voss et al. 2017; Xie et al. 2020). Key observations are the shortening of SSE recurrence intervals may decrease with time like empirical afterslip-driven sequences, e.g., aftershocks (Hsu et al. 2006) and creep events (Wei et al. 2015). In the southernmost Ryukyu subduction zone, the SSEs increase to intervals of 3.1, 4.2, and 6.2 years after the 2002 M_w 7.1 Hualien offshore earthquake. The increasing SSE intervals with a decreasing shortening seem similar to the evolution of postseismic displacements (Fig. 3). But the observation is different to the Boso SSEs that increase to intervals of 0.6, 2.2, and then 4.4 years after the M_w 9.0 Tohoku earthquake (Luo and Liu 2019; Ozawa et al. 2019). The first and second Boso SSEs showed much more shortening than the SSEs in our study area. The amount of shortening SSE intervals along with afterslip may be controlled by earthquake size and corresponding stress perturbations (Luo and Liu 2019). The larger the earthquake size is, the greater the amount of shortening SSE intervals will be. It might explain a smaller amount of the first SSE shortening interval from this study (Fig. 1a). It might also explain the shortening

SSE intervals decrease slowly with time in the M_w 7.1 case. A weaker afterslip following the M_w 7.1 earthquake size than the M_w 9.0 one could be a reason. Note that the increasing recurrence intervals of the Boso SSEs in Japan recurred on the same fault patch. This patch is not overlapped by the afterslip region of the M_w 9.0 Tohoku earthquake but is close enough. Our results indicate that the afterslip region of the 2002 M_w 7.1 Hualien offshore earthquake very likely overlapped the SSE regions. The close relation makes the influence of afterslip on SSE sequence more reasonable observed with positive coseismic and postseismic stress loads. Thus, SSEs at the edge or even within the afterslip region may be triggered when the SSE region is approaching a triggering stress level. This interpretation does not limit the observations to the repeating SSEs on the same fault patch. Continuous monitoring of future SSEs in our study region and the Boso region in Japan would understand the discrepancy.

Conclusions

We report an increase of SSEs intervals after a large earthquake in the southernmost Ryukyu subduction zone, similar to the Boso SSEs observation in Japan. The 2005 SSE region and the 2009/2015 repeating SSEs region are very likely influenced by afterslip from the 2002 M_w 7.1 Hualien offshore earthquake. The coseismic and postseismic Coulomb stress changes on the 2005 SSE region were significant than the 2009/2015 repeating SSEs region. The number of positive stress changes and postseismic decelerated stress evolution can suitably explain the increasing SSE intervals. If the postseismic decelerated stress lasted at least till early 2007, the 2005 SSE was likely triggered by the M_w 7.1 earthquake afterslip. The 2009 SSE is suspected to be affected by the afterslip as well. The different SSE timings may be due to variable frictional properties or stressed levels on the two SSE regions. Our study provides insights into the linkage from postseismic stress evolution, frictional and stressed conditions of the SSEs region to SSEs recurrence intervals.

List Of Abbreviations

SSEs: slow slip events; ISZ: the interplate seismogenic zone; SSZ: slow slip zone; GNSS: Global Navigation Satellite System; EQ: earthquake; M_w: moment magnitude; M_L: local magnitude; GPa: gigapascal MPa: megapascal

Declarations

Ethics approval and consent to participate

not applicable

Consent for publication

not applicable

Availability of data and materials

The GNSS data are available at http://gps.earth.sinica.edu.tw/. The Coulomb stress calculations were performed using Coulomb 3 software, available from https://www.usgs.gov/software/coulomb-3.

Competing interests

The authors declare that they have no competing interests.

Funding

This study was funded by the Ministry of Science and Technology (MOST) in Taiwan under grant number 109-2116-M-002-030-MY3 and 106-2116-M-002-019-MY3.

Authors' contributions

SK Chen analyzed the data, SK Chen, YM Wu and YC Chan wrote the manuscript. All authors read and approved the final manuscript.

Acknowledgements

We acknowledge the Institute of Earth Sciences, Academia Sinica, Taiwan for providing the GNSS data.

References

1. Bürgmann, R (2018) The geophysics, geology and mechanics of slow fault slip. Earth Planet Sci Lett 495:112–134. https://doi.org/10.1016/j.epsl.2018.04.062
2. Chen, HY, Kuo, LC, Yu, SB (2004) Coseismic movement and seismic ground motion associated with the 31 March 2002 off Hualien, Taiwan, Earthquake. Terr Atmos Ocean Sci 15:683–695. https://doi.org/10.3319/TAO.2004.15.4.683(T)
3. Chen, SK, Chan, YC, Hu, JC, Kuo, LC (2014) Current crustal deformation at the junction of collision to subduction around the Hualien area, Taiwan. Tectonophysics 617:58-78. https://doi.org/10.1016/j.tecto.2014.01.014
4. Chen, SK, Wu, YM, Hsu, YJ, Chan, YC (2017) Current crustal deformation of the Taiwan orogen reassessed by cGPS strain-rate estimation and focal mechanism stress inversion. *Geophys J Int* 210:228–239. https://doi.org/10.1093/gji/ggx165
5. Chen, SK, Wu, YM, Chan, YC (2018) Episodic slow slip events and overlying plate seismicity at the southernmost Ryukyu Trench. Geophys Res Lett 45:10,369–10,377. https://doi.org/10.1029/2018GL079740
6. Cheng, SN, Yeh, YT (1989) Catalog of the earthquakes in Taiwan from 1604 to 1988. *Bulletin IES*, R-661, 255pp., Institute of Earth Sciences, Taipei.
7. Dixon TH, Jiang Y, Malservisi R, McCaffrey R, Voss N, Protti M, Gonzalez V (2014) Earthquake and tsunami forecasts: relation of slow slip events to subse-quent earthquake rupture. Proc Natl Acad Sci 111:17039–17044. https://doi.org/10.1073/pnas.1412299111

8. Hirose H, Kimura H, Bogdan Enescu B, Aoi S (2012) Recurrent slow slip event likely hastened by the 2011 Tohoku earthquake. Proc Natl Acad Sci 109:15157–15161. https://doi.org/10.1073/pnas.1202709109
9. Hsu YJ, Simons M, Avouac JP, Galetzka J, Sieh K, Chlieh M, Natawidjaja D, Prawirodirdjo L, Bock Y (2006) Frictional afterslip following the 2005 Nias-Simeulue earthquake, Sumatra. Science 312:1921–1926. https://doi.org/10.1126/science.1126960
10. Hsu YJ, Yu SB, Simons M, Kuo LC, Chen HY (2009) Interseismic crustal deformation in the Taiwan plate boundary zone revealed by GPS observations, seismicity, and earthquake focal mechanisms. Tectonophysics 479:4–18. https://doi.org/10.1016/j.tecto.2008.11.016
11. Hsu YJ, Ando M, Yu SB, Simons M (2012) The potential for a great earthquake along the southernmost Ryukyu subduction zone. Geophys Res Lett 39:L14302. https://doi.org/10.1029/2012GL052764
12. Hu Y, Bürgmann R, Uchida N, Banerjee P, Freymueller JT (2016) Stress-driven relaxation of heterogeneous upper mantle and time-dependent afterslip following the 2011 Tohoku earthquake. J Geophys Res 121:385–411. https://doi.org/10.1002/2015JB012508
13. Huang HH., Wu YM., Song XD, Chang CH, Lee SC, Chang TM, Hsieh HH (2014). Joint V_P and V_S tomography of Taiwan: implications for subduction-collision orogeny. Earth Planet Sci Lett 392:177–191. https://doi.org/10.1016/j.epsl.2014.02.026
14. Ikari MJ, Kopf AJ, Hüpers A, Vogt C (2018) Lithologic control of frictional strength variations in subduction zone sediment inputs. Geosphere 14:604–625. https://doi.org/10.1130/GES01546.1
15. Ito Y, Hino R, Kido M, Fujimoto H, Osada Y, Inazu D et al. (2013) Episodic slow slip events in the Japan subduction zone before the 2011 Tohoku-Oki earth-quake. Tectonophysics 600:14–26. https://doi.org/10.1016/j.tecto.2012.08.022
16. Kaneki S, Hirono T (2019) Diagenetic and shear-induced transitions of frictional strength of carbon-bearing faults and their implications for earthquake rupture dynamics in subduction zones. Sci Rep 9:7884. https://doi.org/10.1038/s41598-019-44307-y
17. Katakami S, Kaneko Y, Ito Y, Araki E (2020) Stress sensitivity of instantaneous dynamic triggering of shallow slow slip events. J Geophys Res 125: e2019JB019178. https://doi.org/10.1029/2019JB019178
18. Kao H (1998) Can great earthquakes occur in the southernmost Ryukyu arc-Taiwan region? Terr Atmos Ocean Sci 9:487–508. https://doi.org/10.3319/TAO.1998.9.3.487
19. King GCP, Stein RS, Lin J (1994) Static stress changes and the triggering of earthquakes. Bull Seis Soc Am 84:935–953.
20. Lee SJ, Dimitri Komatitsch, D, Huang BS, Tromp J (2009) Effects of Topography on Seismic-Wave Propagation: An Example from Northern Taiwan. Bull Seis Soc Am 99:314–325. https://doi.org/10.1785/0120080020
21. Luo Y, Liu Z (2019) Slow-slip recurrent pattern changes: perturbation responding and possible scenarios of precursor toward a megathrust earthquake. Geochem Geophys Geosys 20:852–871.

https://doi.org/10.1029/2018GC008021

22. Matsuzawa T, Hirose H, Shibazaki B, Obara K (2010) Modeling short-and long-term slow slip events in the seismic cycles of large subduction earthquakes. J Geophys Res 115:B12301. https://doi.org/10.1029/2010JB007566
23. Matsuzawa T, Shibazaki B, Obara K, Hirose H (2013) Comprehensive model of short-and long-term slow slip events in the Shikoku region of Japan, incorporating a realistic plate configuration. Geophys Res Lett 40:5125–5130. https://doi.org/10.1002/grl.51006
24. Nakamura M (2009) Aseismic crustal movement in southern Ryukyu Trench, southwest Japan. Geophys Res Lett 36:L20312, http://doi.org/10.1029/2009GL040357
25. Namiki Y, Tsutsumi A, Ujiie K, Kameda J (2014) Frictional properties of sediments entering the Costa Rica subduction zone offshore the Osa Peninsula: Implications for fault slip in shallow subduction zones. Earth Planets Space 66:72, https://doi.org/10.1186/1880-5981-66-72
26. Nishimura S, Hashimoto M, Ando M (2004) A rigid block rotation model for the GPS derived velocity field along the Ryukyu arc. Phys Earth Planet Int 142:185–203. https://doi.org/10.1016/j.pepi.2003.12.014
27. Obara K, Kato A (2016) Connecting slow earthquakes to huge earthquakes. Science 353:253–257. https://doi.org/10.1126/science.aaf1512
28. Okada Y (1992) Internal deformation due to shear and tensile faults in a half-space. Bull Seis Soc Am 82:1018–1040.
29. Ozawa S, Suito H, Tobita M (2007) Occurrence of quasi-periodic slow slip off the east coast of the Boso peninsula, central Japan. Earth Planets Space 59:1241–1245. https://doi.org/10.1186/BF03352072
30. Ozawa S, Yarai H, Kobayashi T (2019) Recovery of the recurrence interval of Boso slow slip events in Japan. Earth Planets Space 71:78. https://doi.org/10.1186/s40623-019-1058-y
31. Rogers G, Dragert H (2003) Episodic tremor and slip on the Cascadia subduction zone: the chatter of silent slip. Science 330:1942–1943. https://doi.org/10.1126/science.1084783
32. Saffer DM, Wallace LM (2015) The frictional, hydrologic, metamorphic and thermal habitat of shallow slow earthquakes. Nat Geo 8:594–600. https://doi.org/10.1038/ngeo2490
33. Scholz CH (2015) On the stress dependence of the earthquake b value. Geophys Res Lett 42:1399–1402. https://doi.org/10.1002/2014GL062863
34. Schwartz SY, Rokosky JM (2007) Slow slip events and seismic tremor at circum-Pacific subduction zones. Rev Geophys 45:RG3004. https://doi.org/10.1029/2006RG000208
35. Segall P. Bradley AM (2012) Slow-slip evolves into megathrust earthquakes in 2D numerical simulations. Geophys Res Lett 39:L18308. https://doi.org/10.1029/2012GL052811
36. Shibazaki B, Wallace LM, Kaneko Y, Hamling I, Ito Y, Matsuzawa T (2019). Three-dimensional modeling of spontaneous and triggered slow-slip events at the Hikurangi subduction zone, New Zealand. J Geophys Res 124:13250–13268. https://doi.org/10.1029/2019JB018190

37. Sibuet JC, Letouzey J, Barbier F, Charvet J, Foucher JP, Hilde TWC, et al. (1987) Back arc extension in the Okinawa trough. J Geophys Res 92:14,041–14,063. https://doi.org/10.1029/JB092iB13p14041
38. Stein RS (1999) The role of stress transfer in earthquake occurrence. Nature 402:605–609. https://doi.org/10.1038/45144
39. Theunissen T, Font Y, Lallemand S, Liang WT (2010) The largest instrumentally recorded earthquake in Taiwan: Revised location and magnitude, and tectonic significance of the 1920 event. *Geophys J Int* 183:1119–1133. https://doi.org/10.1111/j.1365-246X.2010.04813.x
40. Toda S, Stein RS, Sevilgen V, Lin J (2011) Coulomb 3.3 Graphic-rich deformation and stress-change software for earthquake, tectonic, and volcano research and teaching–user guide. In: U.S. Geological Survey Open-File Report 2011–1060, 63 p., available at. https://pubs.usgs.gov/of/2011/1060
41. Voss N, Malservisi R, Dixon TH, Protti M (2017) Slow slip events in the early part of the earthquake cycle. J Geophys Res 122:6773–6786. https://doi.org/10.1002/2016JB013741
42. Wang K, Hu Y, He J (2012) Deformation cycles of subduction earthquakes in a viscoelastic Earth. Nature 484:327–332. https://doi.org/10.1038/nature11032
43. Wallace LM, Kaneko Y, Hreinsdóttir S, Hamling I, Peng Z, Bartlow N, D'Anastasio E, Fry B (2017) Large-scale dynamic triggering of shallow slow slip enhanced by overlying sedimentary wedge. Nat Geo 10:765–770. https://doi.org/10.1038/ngeo3021
44. Wallace LM, Hreinsdóttir S, Ellis S, Hamling I, D'Anastasio E, Denys P (2018) Triggered slow slip and afterslip on the southern Hikurangi subduction zone following the Kaikōura earthquake. Geophys Res Lett 45:4710–4718. https://doi.org/10.1002/2018GL077385
45. Wei M, Liu Y, Kaneko Y, McGuire JJ, Bilham R (2015) Dynamic triggering of creep events in the Salton Trough, Southern California by regional M ≥ 5.4 earthquakes constrained by geodetic observations and numerical simulations. Earth Planet Sci Lett 532:115970. https://doi.org/10.1016/j.epsl.2019.115970
46. Wei M, Kaneko Y, Shi P, Liu Y (2018). Numerical modeling of dynamically triggered shallow slow slip events in New Zealand by the 2016 M_w 7.8 Kaikoura earthquake. Geophys Res Lett 45:4764–4772. https://doi.org/10.1029/2018GL077879
47. Wu YM, Chang CH, Zhao L, Teng TL, Nakamura M (2008) A comprehensive relocation of earthquakes in Taiwan from 1991 to 2005. Bull Seis Soc Am 98:1471–1481. https://doi.org/10.1785/0120070166
48. Wu YM, Shyu JBH, Chang CH, Zhao L, Nakamura M, Hsu SK (2009) Improved seismic tomography offshore northeastern Taiwan: implications for subduction and collision processes between Taiwan and the southernmost Ryukyu. *Geophys J Int* 178:1042–1054. https://doi.org/10.1111/j.1365-246X.2009.04180.x
49. Wu YM, Chen SK, Huang TC, Huang HH, Chao WA, Koulakov I (2018) Relationship between earthquake b-values and crustal stresses in a young orogenic belt. Geophys Res Lett 45:1832–1837. https://doi/10.1002/2017GL076694

50. Xie S, Dixon TH, Malservisi R, Jiang Y, Protti M, Muller C (2020) Slow slip and inter-transient locking on the Nicoya megathrust in the late and early stages of an earthquake cycle. J Geophys Res 125:e2020JB020503 https://doi.org/10.1029/2020JB020503

Figures

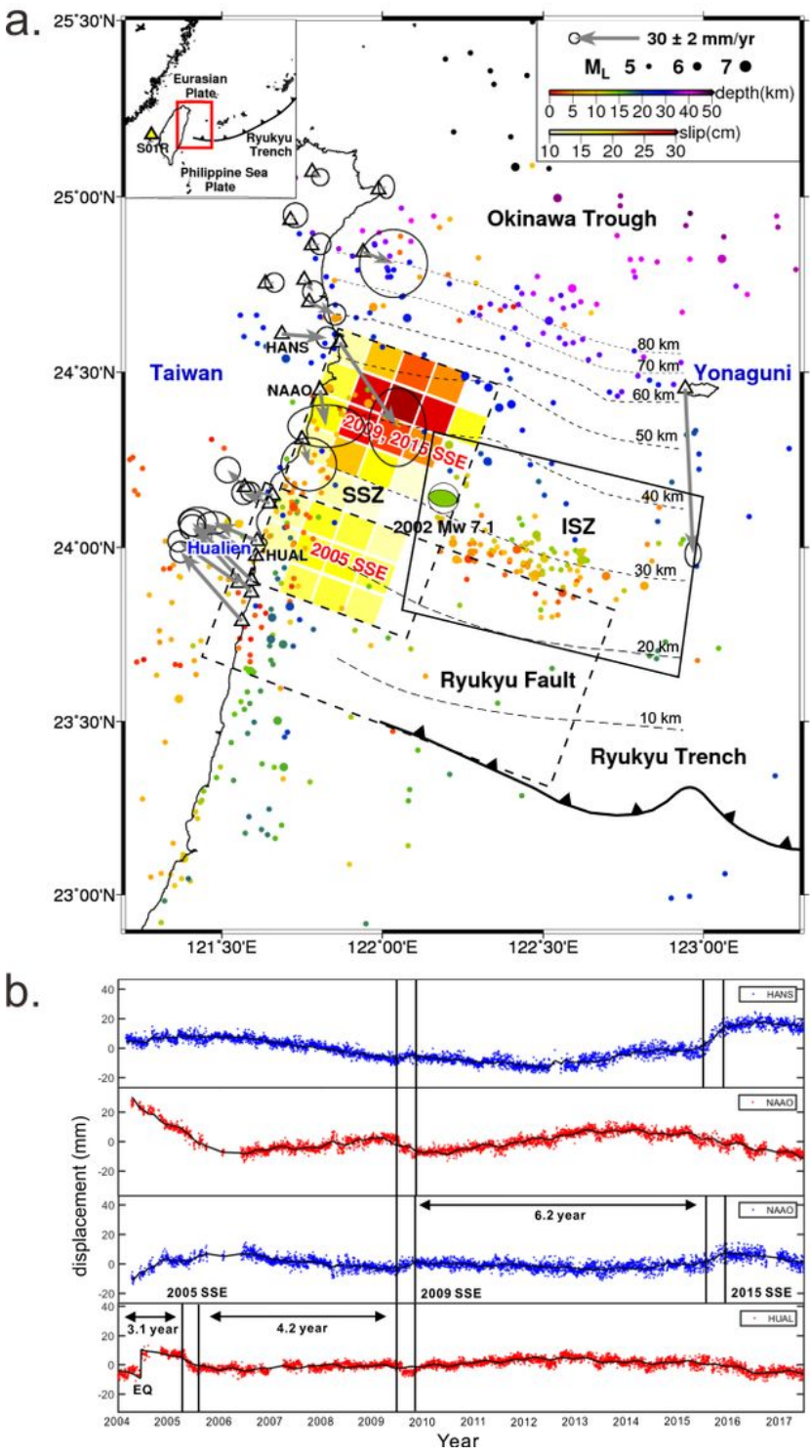

Figure 1

Tectonics, seismicity, and slow slip events of the southernmost Ryukyu subduction zone. a. ISZ: Interplate Seismogenic Zone; SSZ: Slow Slip Zone, with cumulative slip during slow slip events (Chen et al., 2018); and Ryukyu Fault. Dotted rectangles represent the possible maximal sizes. Horizontal surface deformation (gray arrows) at each GNSS station (white triangles) is based on the S01R station (yellow triangle). Relocated seismicity from 1991 to 2018 (Wu et al. 2008) is colored for depth. The depths along the subduction interface are derived from local seismic tomography (Wu et al. 2009). b. GNSS time series and timings of SSEs. The blue and red position time series represent the east and north components, respectively. The locations of the GNSS stations are marked in Fig. 1a. Each slow-slip interval is shown after the 2002 Mw 7.1 earthquake. EQ: coseismic offset by a 2004 local ML 5.8 earthquake. Note: The designations employed and the presentation of the material on this map do not imply the expression of any opinion whatsoever on the part of Research Square concerning the legal status of any country, territory, city or area or of its authorities, or concerning the delimitation of its frontiers or boundaries. This map has been provided by the authors.

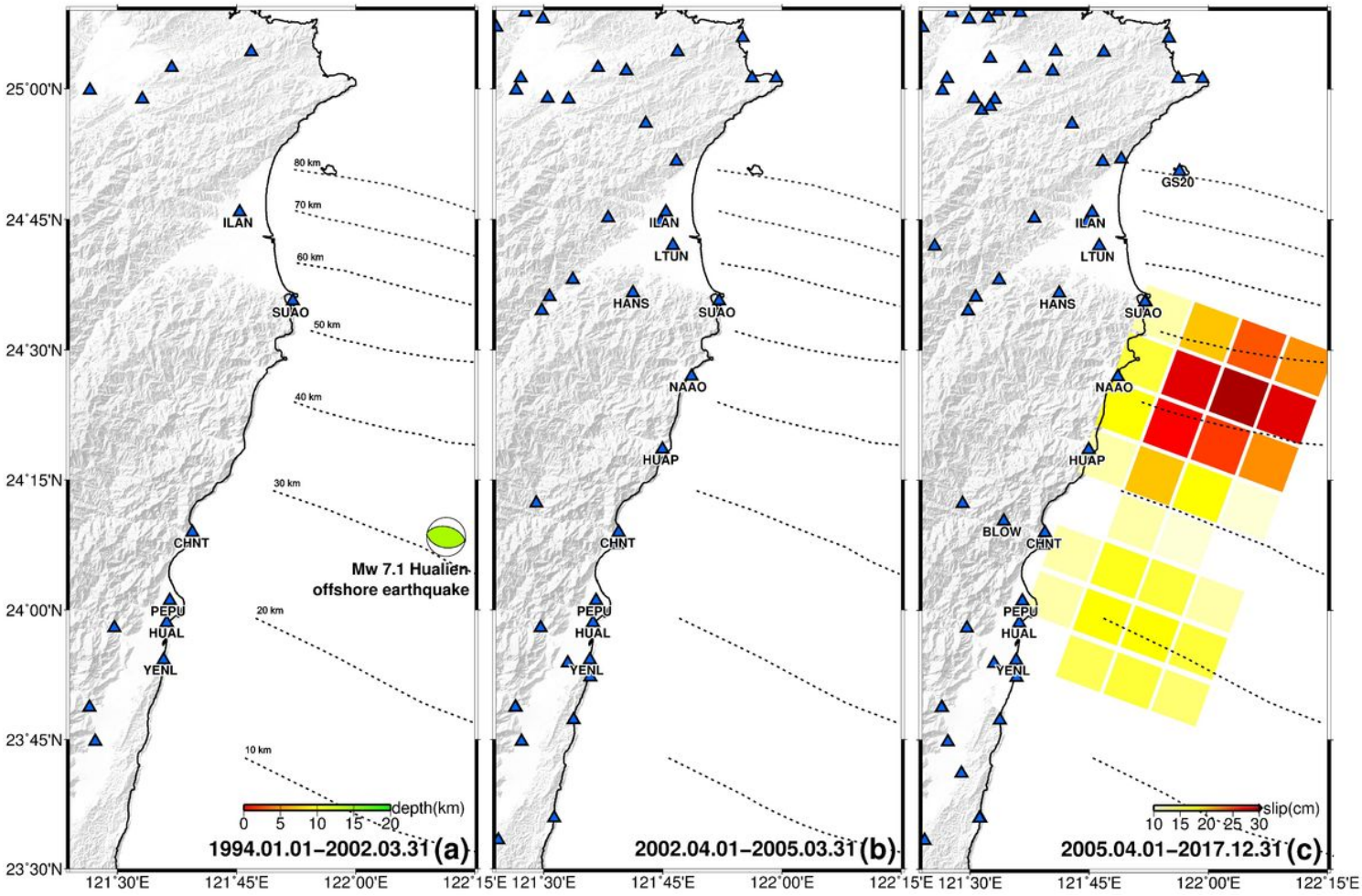

Figure 2

Three-period GNSS station distribution in the eastern Taiwan region. The periods before (a) and after (b) the 2002 Mw 7.1 Hualien offshore earthquake and after the 2005 slow slip event (c) are shown individually. GNSS stations (blue triangles) near the source region of slow slip events are named in each subplot. Note: The designations employed and the presentation of the material on this map do not imply

the expression of any opinion whatsoever on the part of Research Square concerning the legal status of any country, territory, city or area or of its authorities, or concerning the delimitation of its frontiers or boundaries. This map has been provided by the authors.

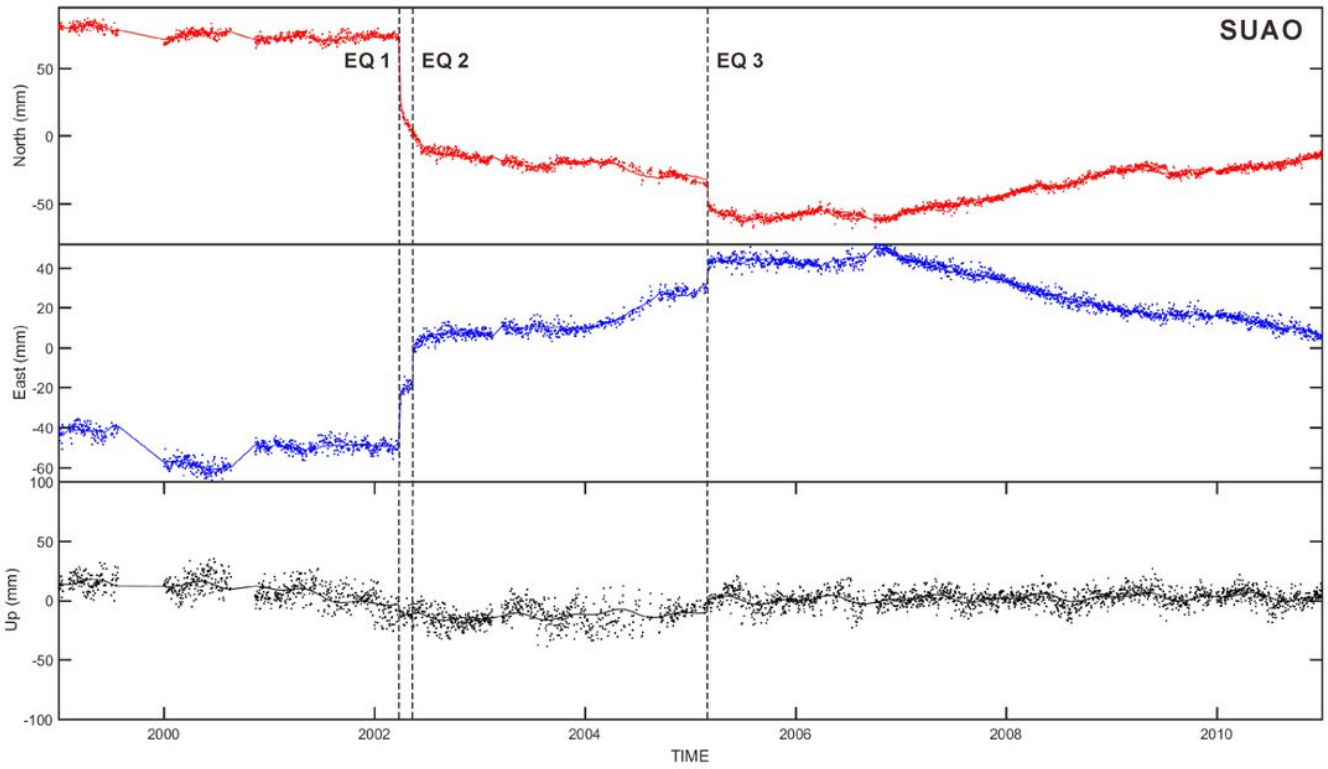

Figure 3

Coseismic and postseismic displacements by the EQ 1 at the nearest SUAO station. The location of the SUAO station is marked in Fig. 1. EQ 1: coseismic offset by the 2002 Mw 7.1 Hualien offshore earthquake. EQ 2: coseismic offset by a local Mw 6.0 Suao earthquake. EQ3: coseismic offset by local Mw 5.9 Ilan doublet earthquakes. Note: The designations employed and the presentation of the material on this map do not imply the expression of any opinion whatsoever on the part of Research Square concerning the legal status of any country, territory, city or area or of its authorities, or concerning the delimitation of its frontiers or boundaries. This map has been provided by the authors.

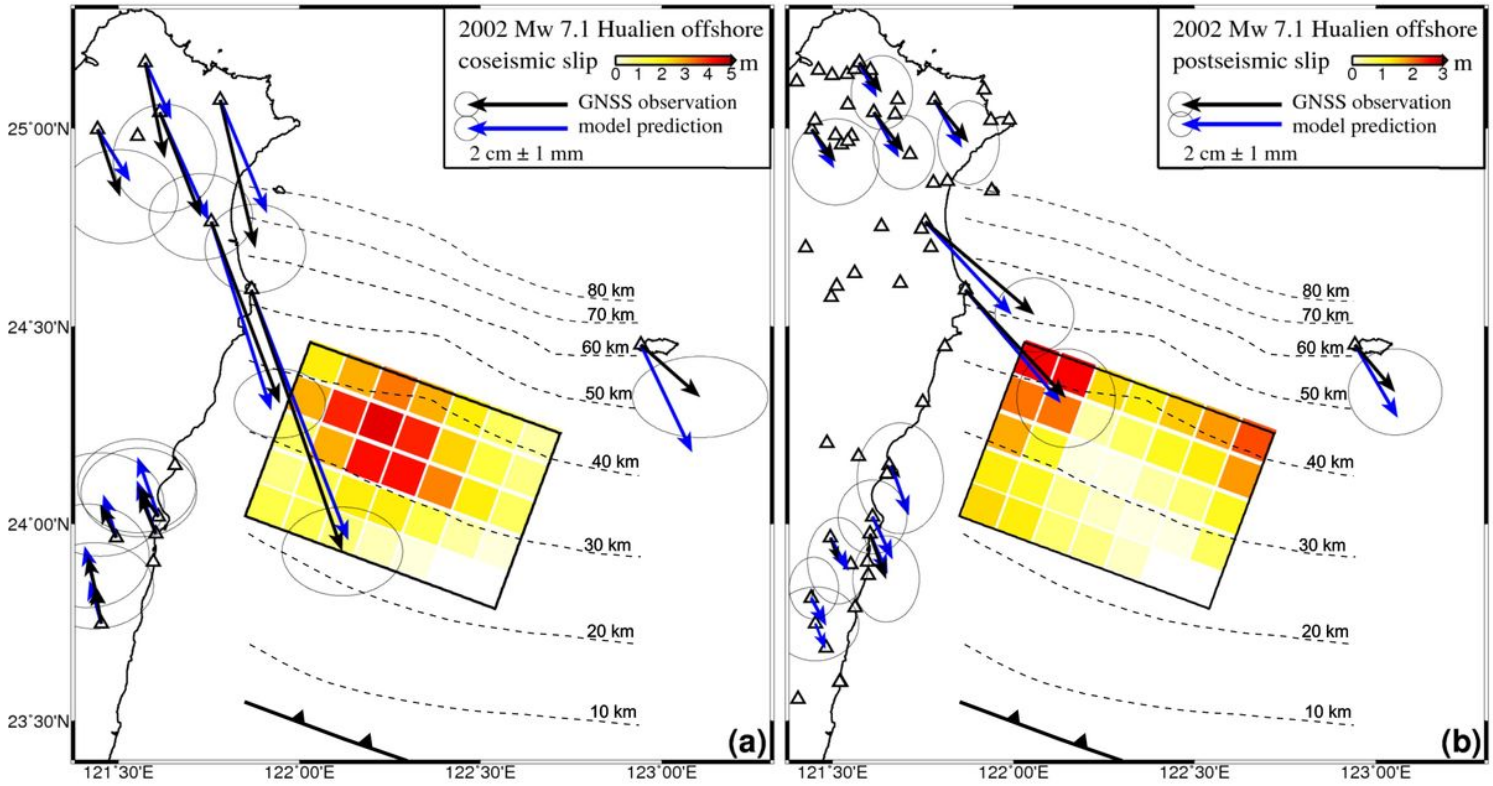

Figure 4

Coseismic slip and afterslip of the 2002 Mw 7.1 Hualien offshore earthquake. The fault dimension and slip are shown by black rectangles and color bars, respectively. The white triangles represent the onshore GNSS stations before (a) and after (b) the Mw 7.1 earthquake. Note: The designations employed and the presentation of the material on this map do not imply the expression of any opinion whatsoever on the part of Research Square concerning the legal status of any country, territory, city or area or of its authorities, or concerning the delimitation of its frontiers or boundaries. This map has been provided by the authors.

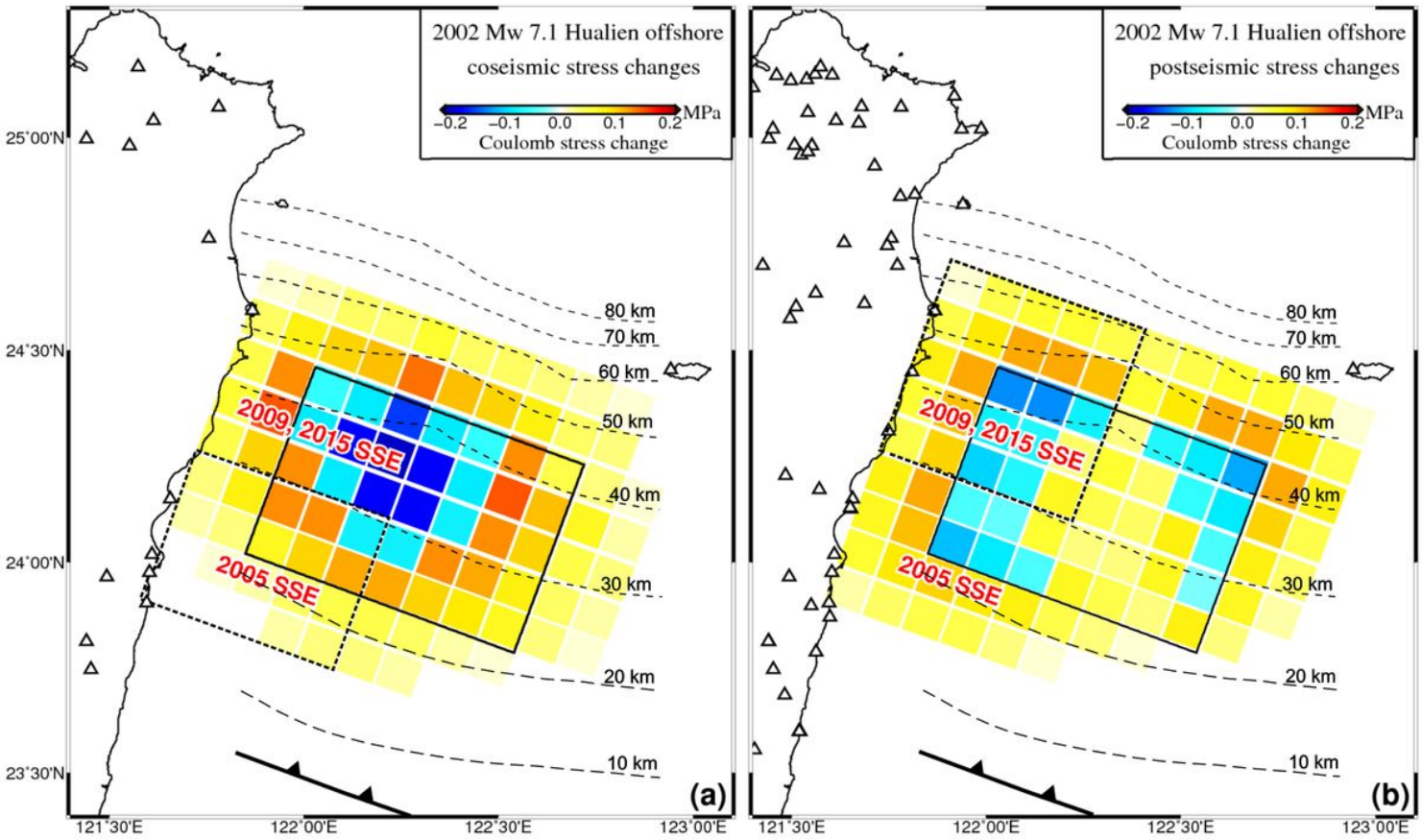

Figure 5

Coseismic (a) and postseismic (b) Coulomb stress changes based on Figure 4. Solid and dotted rectangles represent the Mw 7.1 earthquake's fault plane and the two slow-slip zones, respectively. Note: The designations employed and the presentation of the material on this map do not imply the expression of any opinion whatsoever on the part of Research Square concerning the legal status of any country, territory, city or area or of its authorities, or concerning the delimitation of its frontiers or boundaries. This map has been provided by the authors.

Supplementary Files

This is a list of supplementary files associated with this preprint. Click to download.

- GraphicalAbstract.jpg